# ARTICLES

## Theoretical Study of CO and NO Vibrational Frequencies in Cu−Water Clusters and Implications for Cu-Exchanged Zeolites

**R. Ramprasad,[†] W. F. Schneider,[‡] K. C. Hass,*[,‡] and J. B. Adams[†,§]**

*Department of Materials Science and Engineering, University of Illinois, Urbana, Illinois 61801, and Ford Research Laboratory, MD 3028/SRL, Dearborn, Michigan 48121-2053*

*Received: May 21, 1996; In Final Form: December 23, 1996*[⊗]

Local spin density functional theory calculations of vibrational frequencies were performed for small Cu-containing complexes in an effort to assess models of exchanged Cu ion sites in zeolites and to help interpret infrared spectroscopy results. Model complexes consisted of $Cu^{n+}$ ($n = 0-2$) ions with varying coordination to water ligands and to more realistic fragments of zeolites. Calculated CO and NO vibrational frequencies for Cu-bound mono- and dicarbonyl and mono- and dinitrosyl species lie in ranges consistent with experimentally observed frequencies and confirm earlier assignments. Our results show a clear linear correlation between bond length and frequency for both carbonyl and nitrosyl complexes. The (nominal) oxidation state of Cu in these complexes is the most important factor in determining CO and NO frequencies and bond lengths, with the local coordination of Cu and the presence of explicit countercharges producing secondary effects.

### I. Introduction

Cu-exchanged zeolites, particularly ZSM-5, show considerable promise both for the selective catalytic reduction (SCR) and decomposition of NO.[1−3] In order to understand this facile catalytic activity, several researchers have used infrared spectroscopy to probe the adsorption of NO on oxidized and reduced forms of various Cu-exchanged zeolites (such as ZSM-5, UHSY, mordenite, erionite, and Y).[4−14] The vibrational spectrum of NO adsorbed on the oxidized form of the catalyst (which contains predominantly $Cu^{2+}$ ions) displays two bands at 1895 and 1912 $cm^{-1}$, which have been assigned to the stretching modes of NO coordinated to a $Cu^{2+}$ ion near one and two framework Al atoms, respectively.[7,8] The vibrational spectrum of NO adsorbed on the reduced form of the catalyst (containing predominantly $Cu^{+}$ ions) includes a band at 1810−1812 $cm^{-1}$ assigned[4−11] to a single NO on $Cu^{+}$ and bands at 1824−1827 and 1729−1735 $cm^{-1}$ assigned to the symmetric and antisymmetric NO stretch of *gem* dinitrosyl species coordinated to $Cu^{+}$, respectively.[4−11] Despite the availability of a wealth of infrared and other experimental information,[15−26] the geometric details of these species and the issue of whether they are spectators or intermediates in various catalytic reactions remains largely unresolved.

Recently, we reported[27] a density functional theory study of Cu binding and NO and CO interaction with Cu ions in small cluster models of Cu-exchanged zeolites. Because the local coordination environment of exchanged Cu ions in high silica zeolites like ZSM-5 is not well-known, and may not even be static under all conditions, we chose to focus on extremely simple models that provide general insights, rather than more elaborate models that introduce additional assumptions and are less amenable to systematic analysis. In the simplest of our models, the zeolite oxygen atoms that coordinate directly to the Cu ion are represented by water ligands, while the remainder of the zeolite lattice is neglected. Thus, for example, a Cu ion in a locally anionic, approximately 4-fold zeolite coordination site becomes a Cu ion coordinated to four suitably oriented, neutral water ligands. This model clearly neglects some of the important features of the true zeolite coordination environment, such as the topology of the zeolite, the local zeolite charge introduced by Al substitution, and the long-range electrostatic field of the zeolite; it thus cannot be expected *a priori* to provide a quantitatively accurate description of the chemistry of zeolite-bound Cu ions. However, it does reasonably represent the dominant contributions to the ligand field of the Cu ion, and it is exceedingly useful for exploring the *trends* in molecular and electronic structures and energetics that accompany variations in Cu coordination and oxidation state. In fact, comparisons of the water ligand model with larger, presumably more realistic cluster models of zeolite-bound Cu show that the former actually provides a remarkably robust description of local chemical properties at nominal Cu(0) and Cu(I) sites and at nominal Cu(II) sites with a sufficiently realistic (*i.e.*, high) coordination.[28] Other groups have also recently reported quantum chemical cluster calculations for zeolite-bound Cu ions.[29,30]

In the present work, we extend our density functional theory cluster approach to study the vibrational spectra of CO and NO species adsorbed at exchanged Cu sites. This work complements the growing number of theoretical studies of adsorbate vibrations in zeolites that focus on Brønsted acid sites[32−38] and

* To whom correspondence should be addressed.
[†] University of Illinois.
[‡] Ford Research Laboratory.
[§] Current address: Department of Chemical, Bio and Materials Engineering, Arizona State University, Tempe, AZ 85287.
[⊗] Abstract published in *Advance ACS Abstracts,* February 15, 1997.

S1089-5647(96)01472-1 CCC: $14.00 

at least two prior calculations at the Hartree−Fock level for NO bound to Cu sites.[30,31] We begin by examining the vibrational spectrum of Cu-bound CO in complexes including $[Cu(H_2O)_xCO]^{n+}$, $x = 0, 1, 2, 4$, $n = 0-2$ (water ligand models), and larger, more realistic models[28] (described in the next section), and the corresponding *gem* dicarbonyl complexes $[Cu(H_2O)_x(CO)_2]^{n+}$. CO may play a role in the SCR of NO, and CO has been employed extensively as a spectroscopic probe in studies of Cu-exchanged sites in zeolites.[7,9,15,39,40] Further, the interaction of CO with transition metal ions is well understood theoretically, and the model copper carbonyl complexes provide a ready reference system for our computational study. Next, we examine the analogous NO containing complexes, including $[Cu(H_2O)_xNO]^{n+}$, $x = 0, 1, 2, 4$, $n = 0-2$ (water ligand models), and larger models,[28] and the corresponding *gem* dinitrosyl complexes $[Cu(H_2O)_x(NO)_2]^{n+}$. Throughout this work, we attempt to address the following specific questions: (a) Are the vibrational frequencies calculated using our models consistent with experimentally observed frequencies? (b) Do our results confirm or contradict earlier assignments of observed frequencies? (c) Do modifications of the water ligand model, such as considering larger cluster models, have a significant effect on calculated frequencies? (d) What general factors affect CO and NO frequencies?

## II. Computational Details

All reported calculations were performed using the Amsterdam Density Functional (ADF)[41] code with most options as chosen in ref 27. Within ADF, a single integration mesh parameter controls the numerical accuracy of the Hamiltonian matrix elements; a larger integration mesh parameter increases the computational cost but yields a finer numerical integration mesh and more accurate matrix elements. Because high accuracy is particularly important for frequency calculations,[42] all of the results reported here (both optimized geometries and frequencies) were obtained with a reasonably conservative integration mesh parameter of 4.5. A split-valence plus polarization Slater orbital basis set is used for all main group elements, and a double-zeta s and p and triple-zeta d Slater orbital basis is used for Cu. Equilibrium geometries were obtained within the local spin density approximation (LSDA).[43] Geometries were considered optimized when the maximum and the root-mean-square forces were less than 0.001 hartree/bohr.

The finer integration mesh used here required a reoptimization of the ground state geometries found in ref 27 for monocarbonyl and mononitrosyl complexes; for the most part, this reoptimization produced only minor changes. The Cu in these complexes was coordinated to 0, 1, 2, or 4 water ligands in addition to being coordinated to a single carbonyl or nitrosyl ligand. The complexes themselves were assigned a 0, 1+, or 2+ charge (simulating CO or NO adsorbed to nominal Cu(0), Cu(I), or Cu(II) oxidation states, respectively) and were subjected to certain symmetry restrictions in order to mimic the local environment of Cu ions in zeolites.[27] Additional symmetry constraints were imposed in some cases in order to expedite geometry optimizations; for instance, in all complexes with one water ligand, the Cu, O (of the water ligand), and H atoms were constrained to be in the same plane, and in all complexes with two and four water ligands, all Cu−O bonds were constrained to be equal, as were the O−Cu−X angles and the H−O−Cu−X dihedral angles (X = C or N). While these symmetry constraints are clearly idealizations of the lower symmetry environments present in real zeolites, they allow us to focus on important trends that depend on coordination. CO was found to bind to Cu in a bent fashion in the neutral complexes and linearly in the singly and doubly charged complexes. In the case of mononitrosyl complexes, both linear and bent binding of NO to $Cu^{2+}$ were considered. NO was found to bind in a linear fashion in $[CuNO]^{2+}$ and $[Cu(H_2O)NO]^{2+}$ and preferred bent binding in complexes with two and four water ligands. In $Cu^0$ and $Cu^+$ complexes, NO prefers to bind in a bent fashion. In Tables 1 and 2, we summarize the reoptimized geometries of monocarbonyl and mononitrosyl complexes, respectively.

Larger models of nominal Cu(I) and Cu(II) sites in zeolites that explicitly include framework Si and Al atoms were also considered, as in ref 28. These models were reoptimized using the criteria of the present study together with the symmetry and other geometric constraints imposed previously.[28] Two extreme

**TABLE 1: Selected Geometric Parameters and Scaled EFFF and Full Normal Mode (in Parentheses) CO Stretch Frequencies for $[Cu(H_2O)_x(CO)]^{n+}$ Complexes (Distances in Å, Angles in deg, and Frequencies in $cm^{-1}$)**

| | C−O | Cu−C | Cu−C−O | Cu−O | $\nu_{CO}$ |
|---|---|---|---|---|---|
| | | Cu(0) Systems ($n = 0$) | | | |
| $x = 0$ | 1.152 | 1.867 | 140.5 | | 1966 (1955) |
| $x = 1$ | 1.167 | 1.830 | 143.2 | 1.978 | 1876 (1876) |
| $x = 2$ | 1.171 | 1.810 | 150.2 | 2.122 | 1849 (1857) |
| $x = 4$ | 1.144 | 1.803 | 168.2 | 2.212 | 1985 (2014) |
| expt | | | | | 2108[a] |
| | | Cu(I) Systems ($n = 1$) | | | |
| $x = 0$ | 1.121 | 1.818 | 180.0 | | 2197 (2219) |
| $x = 1$ | 1.124 | 1.784 | 180.0 | 1.870 | 2173 (2198) |
| $x = 2$ | 1.129 | 1.788 | 180.0 | 2.012 | 2130 (2153) |
| $x = 4$ | 1.134 | 1.793 | 180.0 | 2.184 | 2109 (2124) |
| expt | | | | | 2150−2160[b] |
| | | Cu(II) Systems ($n = 2$) | | | |
| $x = 0$ | 1.112 | 1.987 | 180.0 | | 2252 (2276) |
| $x = 1$ | 1.112 | 1.886 | 179.5 | 1.886 | 2257 (2289) |
| $x = 2$ | 1.115 | 1.932 | 180.0 | 1.895 | 2238 (2256) |
| $x = 4$ | 1.118 | 1.869 | 180.0 | 1.999 | 2207 (2214) |
| expt | | | | | 2180[c] |

[a] Cu−ZSM-5.[39] [b] Cu−ZSM-5.[7,9,15,39,40] [c] Cu−ZSM-5.[40]

**TABLE 2: Selected Geometric Parameters and Scaled EFFF and Full Normal Mode (in Parentheses) NO Stretch Frequencies for $[Cu(H_2O)_x(NO)]^{n+}$ Complexes (Distances in Å, Angles in deg, and Frequencies in $cm^{-1}$)**

| | N−O | Cu−N | Cu−N−O | Cu−O | $\nu_{NO}$ |
|---|---|---|---|---|---|
| | | Cu(0) Systems ($n = 0$) | | | |
| $x = 0$ | 1.177 | 1.865 | 118.5 | | 1671 (1648) |
| $x = 1$ | 1.217 | 1.766 | 134.7 | 1.920 | 1522 (1525) |
| $x = 2$ | 1.223 | 1.785 | 136.6 | 2.149 | 1497 (1499) |
| $x = 4$ | 1.234 | 1.824 | 131.0 | 2.314 | 1447 (1427) |
| | | Cu(I) Systems ($n = 1$) | | | |
| $x = 0$ | 1.138 | 1.851 | 127.9 | | 1872 (1854) |
| $x = 1$ | 1.150 | 1.788 | 133.8 | 1.880 | 1853 (1843) |
| $x = 2$ | 1.158 | 1.782 | 139.7 | 1.996 | 1816 (1810) |
| $x = 4$ | 1.168 | 1.830 | 130.4 | 2.172 | 1773 (1760) |
| expt | | | | | 1810−1812[a] |
| | | | | | 1815[b] |
| | | | | | 1810[c] |
| | | Cu(II) Systems ($n = 2$) | | | |
| $x = 0$ | 1.079 | 1.920 | 180.0 | | 2234 (2223) |
| $x = 1$ | 1.089 | 1.756 | 180.0 | 1.840 | 2171 (2181) |
| $x = 2$[d] | 1.096 | 1.764 | 180.0 | 1.935 | 2129 (2137) |
| $x = 2$[e] | 1.092 | 2.187 | 121.4 | 1.870 | 2137 (2121) |
| $x = 4$[d] | 1.098 | 1.790 | 180.0 | 2.098 | 2107 (2115) |
| $x = 4$[e] | 1.104 | 1.903 | 121.9 | 2.080 | 2077 (2057) |
| expt | | | | | 1895, 1909−1912[a] |
| | | | | | 1900, 1950[b] |
| | | | | | 1900[c] |
| | | | | | 1895−1958[f] |
| | | | | | 1895−1946[g] |

[a] Cu−ZSM-5.[4−11] [b] Cu−UHSY.[5] [c] Cu−mordenite.[5] [d] Linear NO. [e] Bent NO. [f] Cu−erionite.[8] [g] Cu−Y.[8,10]

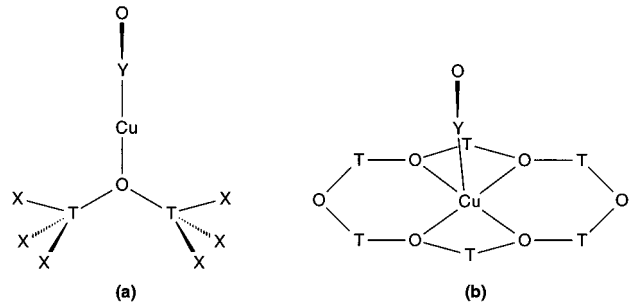


**Figure 1.** Geometries assumed for larger cluster models of (a) 1-coordinated and (b) 4-coordinated Cu. Y = C or N, T = Si, Al, or J, and the T-sites are terminated by either H or OH.

**TABLE 3: Selected Geometric Parameters and Scaled EFFF CO Stretch Frequencies for Larger Model Carbonyl Complexes (Distances in Å and Frequencies in cm$^{-1}$)**

| | C−O | Cu−C | Cu−O | $\nu_{CO}$ |
|---|---|---|---|---|
| Cu(I) Systems | | | | |
| larger models for 1-coordinated Cu | | | | |
| $[Cu(Si_2OH_6)CO]^+$ | 1.124 | 1.786 | 1.896 | 2169 |
| $[Cu(Si_2O(OH)_6)CO]^+$ | 1.126 | 1.784 | 1.921 | 2155 |
| $[Cu(J_2OH_6)CO]$ | 1.133 | 1.754 | 1.836 | 2101 |
| $[Cu(J_2O(OH)_6)CO]$ | 1.134 | 1.755 | 1.852 | 2097 |
| $[Cu(SiAlOH_6)CO]$ | 1.135 | 1.754 | 1.839 | 2078 |
| $[Cu(SiAlO(OH)_6)CO]$ | 1.134 | 1.752 | 1.851 | 2086 |
| larger models for 4-coordinated Cu | | | | |
| $[Cu(Si_6O_6H_{12})CO]^+$ | 1.134 | 1.802 | 2.234 | 2097 |
| $[Cu(Si_4J_2O_6H_{12})CO]$ | 1.138 | 1.794 | 2.209 | 2063 |
| $[Cu(Si_5AlO_6H_{12})CO]^a$ | 1.141 | 1.765 | 2.677 | 2051 |
| | | | 2.002 | |
| Cu(II) Systems | | | | |
| larger models for 4-coordinated Cu | | | | |
| $[Cu(Si_6O_6H_{12})CO]^{2+}$ | 1.125 | 1.843 | 2.172 | 2156 |
| $[Cu(Si_4Al_2O_6H_{12})CO]$ | 1.135 | 1.812 | 2.145 | 2076 |

$^a$ $C_s$ symmetry imposed. Optimized Cu−C−O = 180°.

cases of Cu coordination were considered for nominal Cu(I) sites: Cu bonded to one framework oxygen atom, $[Cu(T_2OX_6)YO]$, X = H or OH, Y = C or N, shown in Figure 1a, and Cu bonded to four framework oxygen atoms, $[Cu(T_6O_6H_{12})YO]$, shown in Figure 1b. Only the relevant high coordination case (Figure 1b) was considered for nominal Cu(II) systems.[28] For purely siliceous clusters, in which all the T sites are occupied by Si atoms, net charges of 1+ and 2+ were imposed to represent nominal Cu(I) and Cu(II), respectively. Neutral cluster models for nominal Cu(I) were constructed by replacing a Si atom by an Al atom or a pair of Si atoms by a pair of hybrid J atoms; neutral nominal Cu(II) models are constructed by replacing two Si atoms by two Al atoms. Each J atom has an atomic number of 13.5, and each pair of J atoms allows a single negative framework charge to be represented without reducing the cluster symmetry. The J atom basis set is constructed by averaging Si and Al basis sets. In Tables 3 and 4, we list selected geometric parameters of the reoptimized larger model complexes.

In addition to monocarbonyl and mononitrosyl complexes, we have also considered dicarbonyl ($[Cu(H_2O)_x(CO)_2]^{n+}$) and dinitrosyl ($[Cu(H_2O)_x(NO)_2]^{n+}$) complexes within the framework of the water ligand model; these are shown in Figures 2 and 3, respectively. All dicarbonyl and dinitrosyl complexes considered were constrained to $C_{2v}$ symmetry (except $[Cu(CO)_2]^{n+}$, $n = 0-2$, which preferred a linear geometry) and were assigned a 0, 1+, or 2+ charge. Cu was coordinated to 0, 1, 2, or 4 water ligands, with the plane of the dicarbonyl or dinitrosyl species between adjacent water ligands ($x > 1$) or between O−H vectors ($x = 1$). In Tables 5 and 6, we list the geometric details of the ground state equilibrium geometries of dicarbonyl and

**TABLE 4: Selected Geometric Parameters and Scaled EFFF NO Stretch Frequencies for Larger Model Nitrosyl Complexes (Distances in Å, Angles in deg, and Frequencies in cm$^{-1}$)**

| | N−O | Cu−N | Cu−N−O | Cu−O | $\nu_{NO}$ |
|---|---|---|---|---|---|
| Cu(I) Systems | | | | | |
| larger models for 1-coordinated Cu | | | | | |
| $[Cu(Si_2OH_6)NO]^+$ | 1.150 | 1.789 | 133.8 | 1.901 | 1848 |
| $[Cu(Si_2O(OH)_6)NO]^+$ | 1.153 | 1.788 | 132.8 | 1.928 | 1838 |
| $[Cu(J_2OH_6)NO]$ | 1.164 | 1.749 | 138.0 | 1.839 | 1781 |
| $[Cu(J_2O(OH)_6)NO]$ | 1.164 | 1.754 | 137.0 | 1.856 | 1782 |
| $[Cu(SiAlOH_6)NO]$ | 1.174 | 1.761 | 136.1 | 1.850 | 1715 |
| $[Cu(SiAlO(OH)_6)NO]$ | 1.175 | 1.767 | 134.3 | 1.868 | 1708 |
| larger models for 4-coordinated Cu | | | | | |
| $[Cu(Si_6O_6H_{12})NO]^+$ | 1.167 | 1.846 | 123.7 | 2.304 | 1774 |
| | | | | 2.169 | |
| $[Cu(Si_4J_2O_6H_{12})NO]$ | 1.173 | 1.842 | 123.2 | 2.269 | 1742 |
| | | | | 2.141 | |
| $[Cu(Si_5AlO_6H_{12})NO]$ | 1.173 | 1.772 | 136.1 | 2.690 | 1736 |
| | | | | 1.988 | |
| Cu(II) Systems | | | | | |
| larger models for 4-coordinated Cu | | | | | |
| $[Cu(Si_6O_6H_{12})NO]^{2+}$ $^a$ | 1.109 | 1.767 | 180.0 | 2.152 | 2017 |
| $[Cu(Si_6O_6H_{12})NO]^{2+}$ $^b$ | 1.119 | 1.860 | 127.4 | 2.134 | 1944 |
| | | | | 2.131 | |
| $[Cu(Si_4Al_2O_6H_{12})NO]$ | 1.135 | 1.831 | 127.2 | 2.128 | 1844 |
| | | | | 2.087 | |

$^a$ Linear NO. $^b$ Bent NO.

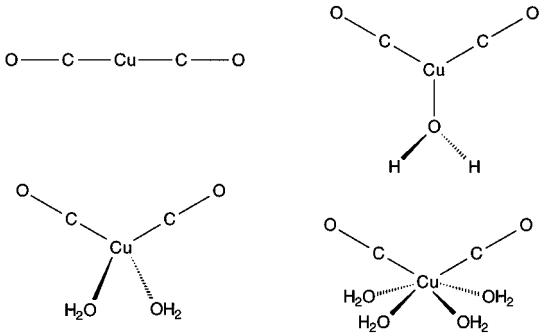

**Figure 2.** Schematic of Cu-bound dicarbonyl $[Cu(H_2O)_x(CO)_2]^{n+}$ complexes for $x = 0$, 1, 2, or 4. Complexes may have overall charge ($n = 0$, 1, or 2) and are all constrained to $C_{2v}$ symmetry except $x = 0$, which has a $D_{\infty h}$ ground state.

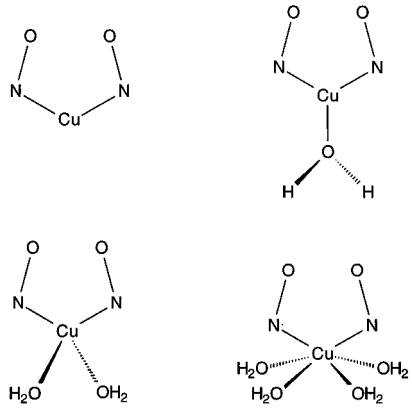

**Figure 3.** Schematic of Cu-bound dinitrosyl $[Cu(H_2O)_x(NO)_2]^{n+}$ complexes for $x = 0$, 1, 2, or 4. Complexes may have overall charge ($n = 0$, 1, or 2) and are all constrained to $C_{2v}$ symmetry.

dinitrosyl complexes, respectively, for which vibrational frequency calculations were performed. A more detailed discussion of the geometric and electronic structure of these complexes and their binding energies will be published elsewhere.[44]

Vibrational frequencies were evaluated using LSDA potential energy surfaces at the LSDA ground state equilibrium geometries. Harmonic frequencies were calculated in all cases using

**TABLE 5: Selected Geometric Parameters and Scaled EFFF and Full Normal Mode (in Parenthesis) Antisymmetric and Symmetric CO Stretch Frequencies for $[Cu(H_2O)_x(CO)_2]^{n+}$ Complexes (Distances in Å, Angles in deg, and Frequencies in $cm^{-1}$)**

| | C−O | Cu−C | Cu−O | C−Cu−C | C−C−O | $\nu^{CO}_{anti}$ | $\nu^{CO}_{sym}$ |
|---|---|---|---|---|---|---|---|
| Cu(0) Systems ($n = 0$) | | | | | | | |
| $x = 0$ | 1.152 | 1.786 | | 180.0 | 180.0 | 1929 (1962) | 2001 (2054) |
| $x = 1$ | 1.156 | 1.791 | 2.139 | 152.7 | 168.2 | 1914 (1945) | 1981 (2028) |
| $x = 2$ | 1.162 | 1.827 | 2.187 | 140.5 | 140.8 | 1861 | 1942 |
| $x = 4$ | 1.160 | 1.820 | 2.606 | 127.1 | 153.6 | 1880 | 1941 |
| Cu(I) Systems ($n = 1$) | | | | | | | |
| $x = 0$ | 1.120 | 1.854 | | 180.0 | 180.0 | 2199 (2205) | 2209 (2242) |
| $x = 1$ | 1.124 | 1.865 | 2.019 | 131.0 | 152.2 | 2162 (2167) | 2177 (2199) |
| $x = 2$ | 1.127 | 1.861 | 2.068 | 123.0 | 148.8 | 2128 | 2147 |
| $x = 4$ | 1.132 | 1.900 | 2.346 | 105.4 | 170.0 | 2093 | 2111 |
| Cu(II) Systems ($n = 2$) | | | | | | | |
| $x = 0$ | 1.112 | 1.966 | | 180.0 | 180.0 | 2261 (2287) | 2262 (2292) |
| $x = 1$ | 1.114 | 1.959 | 1.876 | 97.1 | 136.7 | 2240 (2259) | 2245 (2267) |
| $x = 2$ | 1.116 | 1.978 | 1.979 | 154.2 | 166.8 | 2228 | 2232 |
| $x = 4$ | 1.121 | 1.929 | 2.198 | 98.6 | 139.3 | 2185 | 2190 |
| expt[a] | | | | | | 2150−2151 | 2177−2178 |

[a] Cu−ZSM-5.[7,9]

an approximate "energy-factored force field" (EFFF) method[45,46] and in many cases from a full normal mode analysis as well. The EFFF method assumes that the CO and NO stretch frequencies are decoupled from all the other vibrational modes of the complex;[47] this assumption is justified because the CO and NO frequencies are well separated from the high-frequency O−H, Si−H, Al−H, and J−H modes and the low-frequency Cu−C, Cu−N, Al−O, Si−O, J−O, and Cu−O modes. EFFF calculations for CO and NO stretch modes thus require just two single-point force evaluations in the case of monocarbonyl and mononitrosyl complexes and two single-point force evaluations followed by the (trivial) diagonalization of a $2 \times 2$ matrix in the case of dicarbonyl and dinitrosyl complexes. The single-point forces were calculated for geometries in which the NO and CO bond lengths were stepped from their equilibrium values by $\pm 0.01$ Å. Full normal mode frequencies were calculated in the usual manner within ADF by numerical differentiation of analytic gradients. Some of the full normal mode calculations yield imaginary frequencies for modes that break the imposed symmetry constraints by rotation or twisting of the water molecules. These modes are not points of concern as we are not interested in the global minima of complexes but rather in complexes that provide realistic approximations to the local environments of Cu ions in zeolites.

Comparisons of frequencies calculated by both methods for all monocarbonyl and mononitrosyl complexes and a few dicarbonyl and dinitrosyl complexes (Tables 1, 2, 5, and 6, respectively) indicate generally good agreement between EFFF and normal mode frequencies. The EFFF frequencies can be either higher or lower depending on a competition between (a) the coupling to the lower frequency Cu−Y (Y = C, N) modes, which shifts the Y−O normal mode frequencies upward, and (b) the off-diagonal interaction between Y−O and Cu−Y bonds, which is largely determined by the degree of covalency in these bonds and which shifts the Y−O normal mode frequencies downward.[48] In Cu−YO complexes, normal mode frequencies are generally higher than EFFF results for Y = C (Table 1), but for Y = N, the discrepancies are less systematic (Table 2), probably reflecting greater covalency of the Cu−NO bond. For both ligands, errors in the approximate EFFF frequencies are at most 20−30 $cm^{-1}$ (≈1%). In $Cu-(YO)_2$ complexes, the errors are typically somewhat larger (up to 53 $cm^{-1}$), with CO and NO normal mode frequencies uniformly higher and lower, respectively, than EFFF frequencies (Tables 5 and 6). For the sake of consistency, most of the discussion in this paper focuses on EFFF results, which are the only frequencies we have calculated for our larger zeolite models because of their significantly lower cost compared to full normal mode calculations for these systems. Normal mode results are used *only* when comparing bare $[Cu(YO)_x]^{n+}$ results, $x = 1, 2$, $n = 0-2$, to experiments or to earlier calculations.

Harmonic frequencies calculated by conventional quantum chemistry techniques (*ab initio* and density functional based) tend to overestimate or underestimate the observed frequencies in a systematic manner[49−51] due to the neglect of anharmonicity and incomplete treatment of electron correlation. Introduction of either an overall scaling factor, or a set of scaling factors for different types of modes, can greatly improve agreement between calculated and experimental frequencies.[49,50] Selective scale factors that are specific to the type of system under consideration have also been used.[32] These scale factors are obtained by comparison of calculated frequencies to a small set of robustly assigned observed frequencies. In the present study, we make use of such selective scale factors. Table 7 lists the calculated and experimental vibrational frequencies for CO, $CO^+$, NO, $NO^+$, and $NO^-$. Calculated vibrational frequencies are consistently higher than experimental frequencies by about 3% in nitrosyl species and by about 2% in carbonyl species. In Tables 1−6 and in all subsequent figures, we have therefore scaled the calculated NO stretch frequencies by 0.97 and the CO stretch frequencies by 0.98. Unless otherwise stated, we compare our scaled frequencies with experimentally determined frequencies but compare our unscaled frequencies with other theoretical calculations.

## III. Results and Discussion

**A. $Cu^{n+}$-Bound Monocarbonyl Complexes.** Vibrational frequency calculations were performed for a set of water ligand model complexes in which CO is bonded to Cu in each of its three nominal oxidation states, Cu(0), Cu(I), and Cu(II), and for larger model Cu(I) and Cu(II) monocarbonyl complexes. Tables 1 and 3 list CO stretch frequencies for these cases, as well as experimentally observed frequencies that have been assigned to carbonyl ligands adsorbed at Cu(0), Cu(I), and Cu(II) sites in ZSM-5.[7,9,15,39,40]

Experimental and computational results are available for the triatomics CuCO and $CuCO^+$, comparison with which provides some measure of the expected accuracy of our calculated vibrational frequencies. Our scaled value for CuCO (1955 $cm^{-1}$) is approximately 60 $cm^{-1}$ lower than experimental cryogenic matrix values (2014[55] and 2010 $cm^{-1}$ [56]), a difference that can in part be attributed to the perturbing influence of the matrix. A variety of density functional,[57,58] *ab initio*,[59,60] and hybrid[61] calculations of the CO stretch frequency in CuCO have been reported, which yield unscaled harmonic frequencies from 20 $cm^{-1}$ less (gradient-corrected DFT[57,58]) to more than 70 $cm^{-1}$ greater (second-order Møller−Plesset, modified coupled-pair functional methods[59,60]) than our unscaled result (1995 $cm^{-1}$). Our result is consistent with those calculations of comparable quality. $[CuCO]^+$ has been examined previously with *ab initio* Hartree−Fock[62,63] and coupled-cluster[62] methods; again, our unscaled normal mode result (2264 $cm^{-1}$) is within 30 $cm^{-1}$ of the more accurate coupled-cluster determination. These comparisons indicate that our overall computational approach—and, in fact, *any* computational approach tractable for systems of the size considered here—has at best an accuracy of tens of wavenumbers, even neglecting the uncertainties associated with the models we employ.

The increase in monocarbonyl frequencies with increasing Cu oxidation state for the $[CuCO]^{n+}$ complexes can be

**TABLE 6: Selected Geometric Parameters and Scaled EFFF and Full Normal Mode (in Parentheses) Antisymmetric and Symmetric NO Stretch Frequencies for $[Cu(H_2O)_x(NO)_2]^{n+}$ Complexes (Distances in Å, Angles in deg, and Frequencies in $cm^{-1}$)**

| | N−O | Cu−N | Cu−O | N−Cu−N | N−N−O | $\nu_{anti}^{NO}$ | $\nu_{sym}^{NO}$ |
|---|---|---|---|---|---|---|---|
| | | | | Cu(0) Systems ($n = 0$) | | | |
| $x = 0$ | 1.184 | 1.874 | | 101.6 | 73.8 | 1583 (1539) | 1698 (1699) |
| $x = 1$ | 1.189 | 1.869 | 2.011 | 93.8 | 76.7 | 1564 (1527) | 1690 (1665) |
| $x = 2$ | 1.194 | 1.860 | 2.171 | 93.3 | 77.6 | 1538 | 1670 |
| $x = 4$ | 1.196 | 1.887 | 2.312 | 90.9 | 79.1 | 1519 | 1664 |
| | | | | Cu(I) Systems ($n = 1$) | | | |
| $x = 0$ | 1.141 | 1.947 | | 94.8 | 75.0 | 1828 (1798) | 1890 (1869) |
| $x = 1$ | 1.147 | 1.926 | 1.935 | 89.6 | 77.7 | 1773 (1735) | 1881 (1859) |
| $x = 2$ | 1.153 | 1.899 | 2.032 | 88.2 | 79.4 | 1748 | 1857 |
| $x = 4$ | 1.158 | 1.903 | 2.218 | 88.5 | 79.4 | 1721 | 1831 |
| | | | | Cu(II) Systems ($n = 2$) | | | |
| $x = 0$ | 1.103 | 1.959 | | 140.6 | 122.3 | 2029 (2010) | 2112 (2105) |
| $x = 1$ | 1.111 | 1.968 | 1.896 | 89.8 | 87.9 | 1969 (1940) | 2068 (2056) |
| $x = 2$ | 1.116 | 1.987 | 1.954 | 86.1 | 84.5 | 1930 | 2043 |
| $x = 4$ | 1.121 | 2.028 | 2.163 | 84.8 | 83.2 | 1892 | 1999 |
| expt | | | | | | 1729−1735[a] | 1824−1827[a] |
| | | | | | | 1729[b] | 1825[b] |

[a] Cu−ZSM-5.[4−11] [b] Cu−Y.[8,10]

**TABLE 7: Calculated Equilibrium Bond Lengths and Calculated and Experimental Vibrational Frequencies of Diatomic Molecules in the Gas Phase (Bond Lengths in Å and Frequencies in $cm^{-1}$)**

| | bond length | $\nu_{theory}$ | $\nu_{expt}$ | $\nu_{expt}/\nu_{theory}$ |
|---|---|---|---|---|
| bare CO | 1.131 | 2170 | 2143[a] | 0.988 |
| bare $CO^+$ | 1.114 | 2277 | 2214[b] | 0.972 |
| | scale factor for carbonyl frequencies | | | 0.98 |
| bare NO | 1.154 | 1930 | 1876[c] | 0.972 |
| bare $NO^+$ | 1.063 | 2426 | 2345[c] | 0.967 |
| bare $NO^-$ | 1.286 | 1398 | 1353[c] | 0.968 |
| | scale factor for nitrosyl frequencies | | | 0.97 |

[a] Reference 52. [b] Refernece 53. [c] Reference 54.

understood in terms of charge transfer and orbital mixing considerations. In CuCO, partial charge transfer from the singly occupied Cu 4 s orbital to the CO $2\pi$ antibonding orbital (which is symmetry-allowed only if CuCO is bent) results in a longer CO bond and a decreased CO stretch frequency compared to gaseous CO. In the singly and doubly charged complexes, net electronic charge transfer from the occupied $5\sigma$ antibonding orbital of CO to Cu results in a shorter CO bond and increased CO stretch frequency compared to free CO.

These trends are modified in understandable ways as the Cu coordination is varied. As the coordination to O is increased, the Cu center becomes a better electron donor and poorer electron acceptor and the CO bond tends to lengthen and the CO stretch frequency tends to decrease. The CO stretch frequencies for the 1+ and 2+ complexes (Table 1) lie in almost overlapping, fairly narrow ranges ($<90$ $cm^{-1}$ for 1+ complexes and $<50$ $cm^{-1}$ for 2+ complexes). The neutral $[Cu(H_2O)_n$-CO] complexes exhibit a less regular behavior, associated with the unusually weak carbonyl bonding in these systems; while the C−O bond length and frequency exhibit the expected correlation, they do not vary in a regular fashion with coordination number.

EFFF results for the larger cluster models are tabulated in Table 3 as well. Of all the models listed, the purely siliceous ones are most comparable to the corresponding water ligand models with like coordination and charge. The agreement between the water ligand and the purely siliceous models is excellent in the case of Cu(I) complexes and reasonable in the case of Cu(II) complexes for binding energies,[28] equilibrium geometries, and vibrational frequencies (Tables 1 and 3). The 51 $cm^{-1}$ difference in CO stretch frequencies between $[Cu(H_2O)_4$-$CO]^{2+}$ and $[Cu(Si_6O_6H_{12})CO]^{2+}$ likely reflects the weaker electron-accepting ability of Cu in the larger model. In Cu(I) complexes, inclusion of Al atoms or, to a somewhat lesser extent, pairs of hybrid J atoms in the larger models further decreases the electron-accepting ability of Cu and thus increases the C−O bond length and decreases the CO stretch frequency. For instance, neutral 1- and 4-coordinated Cu(I) complexes display CO stretch frequencies 60−90 and 35−50 $cm^{-1}$ lower, respectively, than those displayed by the corresponding charged Cu(I) complexes. A similar trend is found in Cu(II) systems; neutral $[Cu(Si_4Al_2O_6H_{12})CO]$ yields a frequency that is 80 $cm^{-1}$ lower than $[Cu(Si_6O_6H_{12})CO]^{2+}$.

Clear trends in CO stretch frequencies emerge from these models: a decrease in the Cu oxidation state, an increase in the Cu coordination, and a greater proximity to strong Lewis base sites (like the Al or J atoms of the present study) all tend to shift the CO frequency downward. The same factors determine the C−O bond lengths, and in fact, a linear correlation exists between the calculated bond lengths and stretch frequencies. Figure 4 shows a plot of these quantities for all the water ligand and larger models considered along with the best fit straight line (correlation coefficient 0.9935). Interestingly, the data point corresponding to gas phase CO, which was not used in the fitting procedure, also lies on this best fit line. A similar linear correlation between CO frequency and bond length, based on available experimental data, has been proposed earlier[64] for CO adsorbed on various surfaces of several different metals. However, no definitive relationship between frequency and bond length could be obtained from that study, as the errors in the experimentally determined C−O bond lengths (≈0.1 Å) were of the same order as the correlation that was sought. While bond lengths are more difficult to measure experimentally than frequencies, the latter are more expensive to obtain computationally. In light of these considerations, a certain predictive power can be attributed to the plot in Figure 4, in that, given either the frequency or the bond length, a rough estimate of the other can be readily obtained. Further, shifts in frequencies can be associated with the factors described above.

The ranges of experimental IR absorption frequencies that have previously been assigned to CO adsorbed on Cu(I) and Cu(II) sites in Cu−ZSM-5 are also indicated in Figure 4 and Table 1. As is clearly seen, the two ranges are narrow and separated by only ≈20 $cm^{-1}$, and both fall within the corresponding—but much broader—ranges of calculated frequencies for Cu(I) and Cu(II) carbonyl complexes. The calculated ranges overlap significantly, with the Cu(II) results

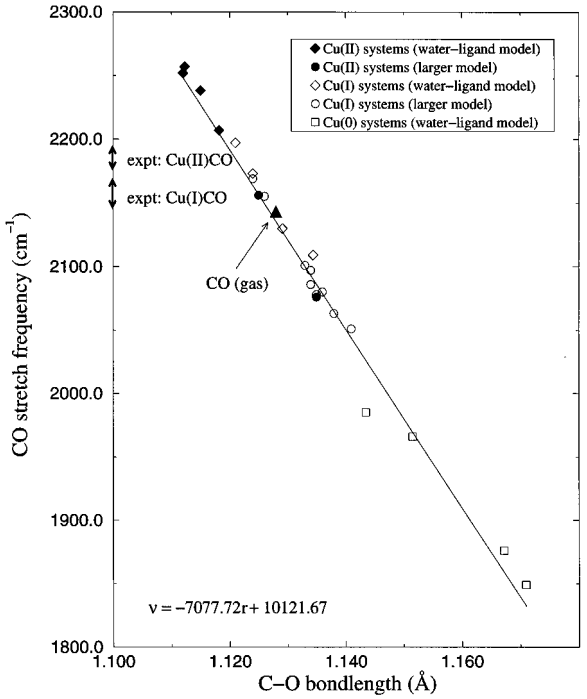


**Figure 4.** Calculated CO frequencies ($\nu$, from EFFF method, scaled by 0.98) vs C−O bond lengths ($r$) for monocarbonyl complexes. Linear fit to data and ranges of experimental values (from Table 1) are also shown.

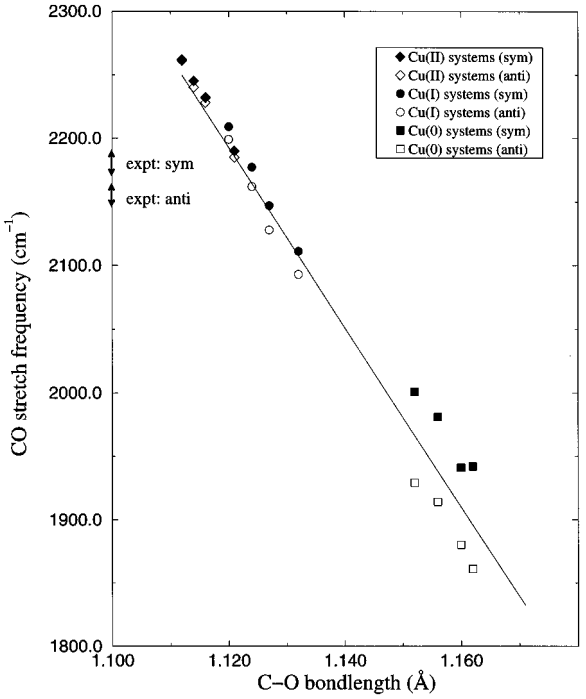


**Figure 5.** Calculated symmetric and antisymmetric CO frequencies (from EFFF method, scaled by 0.98) vs C−O bond lengths for dicarbonyl $[Cu(H_2O)_x(CO)_2]^{n+}$ complexes. Linear fit to monocarbonyl results (from Figure 4) and ranges of experimental values (Table 1) are also shown.

covering a wider range and extending to higher frequency. The small differences between CO frequencies on Cu(I) and Cu(II) reflect a similarity in CO bonding; the slightly higher frequencies for Cu(II) are due to a slightly larger depopulation of the antibonding CO 5$\sigma$ orbital. The better agreement of the water ligand model results with experiments for Cu(I) and Cu(II) is most likely fortuitous. Errors introduced by particular models may be offset to some extent in the present work by uncertainties associated with the assumed transferability of frequency scale factors from gas phase molecules to adsorbates on Cu. Given this situation, and the considerable sensitivity of the calculated CO frequencies to the details of a particular model, it is clearly impossible to make absolute comparisons between calculated and experimental frequencies. Rather, the present results serve to confirm the changes in CO frequency that accompany variations in Cu oxidation state and to indicate the expected shifts in frequency associated with variations in local coordination environment. Our calculated frequencies for CO on *isolated* Cu(0) lie significantly below the experimental value of 2108 cm$^{-1}$ that had tentatively been assigned to this species in Cu−ZSM-5. This discrepancy most likely reflects a clustering of Cu(0) in the sample studied, as 2108 cm$^{-1}$ is much closer to observed frequencies for CO on Cu metal surfaces.[65]

**B. $Cu^{n+}$-Bound Dicarbonyl $[Cu(H_2O)_x(CO)_2]^{n+}$ Complexes.** In studies of CO in Cu-exchanged zeolites, vibrational bands observed at 2150−2151 and 2177−2178 cm$^{-1}$ have been assigned to the antisymmetric and symmetric CO stretch modes, respectively, in dicarbonyl complexes adsorbed at isolated $Cu^+$ sites.[7,9] While dicarbonyl species are unlikely to play a role in the catalytic reduction of NO, they do provide an additional test of our water ligand models. In Table 5, we list the calculated antisymmetric and symmetric CO stretch frequencies in $[Cu(H_2O)_x(CO)_2]^{n+}$ complexes. The IR spectrum of $[Cu_x(CO)_2]$ has been measured in an argon matrix;[56] bands at 1876 and 1891 cm$^{-1}$ have been assigned to the antisymmetric and symmetric CO stretch modes, respectively. Our calculated normal mode frequencies for $[Cu(CO)_2]$ are more than 100 cm$^{-1}$ greater, which likely reflects a difference in Cu stoichiometry in the experiments[56] and calculations. Our unscaled normal mode results for the antisymmetric and symmetric CO stretch modes in $[Cu(CO)_2]$ (2002 and 2096 cm$^{-1}$, respectively) do compare well with Barone's[66] hybrid density functional values of 1998 and 2114 cm$^{-1}$. Hartree−Fock calculations for $[Cu(CO)_2]^+$ [63] yield CO stretch frequencies more than 150 cm$^{-1}$ greater than our (unscaled) normal mode results for this system, reflecting the known systematic overestimation at the Hartree−Fock level.[62]

Figure 5 shows a plot of the EFFF CO (symmetric and antisymmetric) stretch frequencies vs the C−O bond length for dicarbonyl species adsorbed on Cu in each of its three nominal oxidation states. A higher cluster charge (*i.e.*, a higher nominal Cu oxidation state) results in higher stretch frequencies and shorter bond lengths. Also, as in monocarbonyl complexes discussed earlier, a higher degree of coordination makes the Cu center a better electron donor and poorer electron acceptor, resulting in longer CO bonds and lower CO stretch frequencies. The line in Figure 5 is taken directly from the fit to monocarbonyl results in Figure 4. The average of the symmetric and antisymmetric frequencies of the dicarbonyl species has very nearly the same linear dependence on the C−O bond length, regardless of the Cu oxidation state. The splitting between the two CO stretch modes on the other hand increases significantly from Cu(II) to Cu(I) to Cu(0) complexes. The increased coupling with decreasing oxidation state likely reflects the increasing occupation of the CO 2$\pi$ orbitals, which interact strongly with each other. Figure 5 also shows experimentally observed frequencies[7,9] that have been assigned to dicarbonyl species adsorbed on Cu(I) sites in ZSM-5. The present results reinforce this assignment.

**C. $Cu^{n+}$-Bound Mononitrosyl Complexes.** Tables 2 and 4 list NO stretch frequencies for the water ligand and larger model complexes, respectively, along with the experimentally observed frequencies[4−11] assigned to NO bound to the Cu(I)

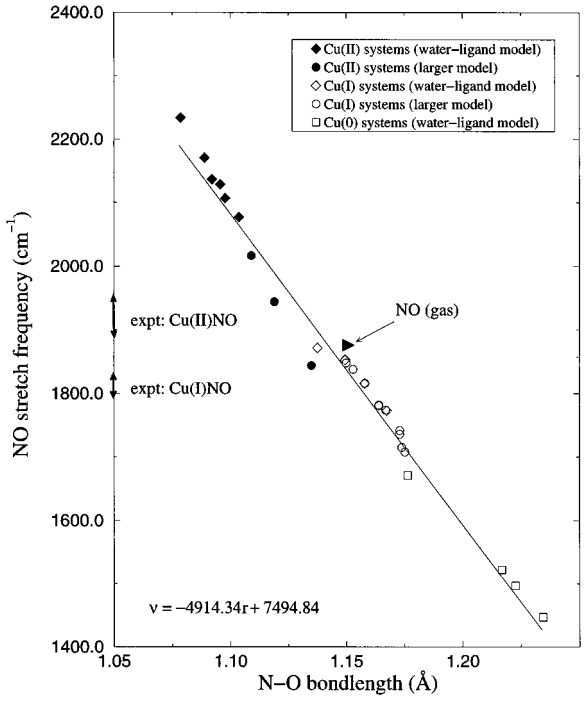


**Figure 6.** Calculated NO frequencies ($\nu$, from EFFF method, scaled by 0.97) vs N−O bond lengths ($r$) for mononitrosyl complexes. Linear fit to data and ranges of experimental values (from Table 2) are also shown.

and Cu(II) sites in Cu-exchanged zeolites. For comparison, previous unrestricted Hartree−Fock calculations for NO bound to nominal Cu(I) sites in cluster models of zeolites yielded NO stretch frequencies of 2231[30] and 1776 cm$^{-1}$.[31] Hartree−Fock vibrational frequencies typically overestimate experimental measurements by about 11%.[50] Application of a standard Hartree−Fock scale factor[50] somewhat improves the former computational result but further increases the discrepancy in the latter.

As discussed previously,[27] in all mononitrosyl complexes, Cu has a strong tendency to exist in an effective Cu(I) oxidation state; *i.e.*, the bonding between NO and Cu$^0$, Cu$^+$ and Cu$^{2+}$ can be approximately represented as [Cu(I)−NO$^-$], [Cu(I)−NO], and [Cu(I)−NO$^+$], respectively. Thus, NO adsorption tends to oxidize Cu$^0$ and reduce Cu$^{2+}$. In CuNO, a partial electron transfer from the Cu 4s level to the antibonding NO 2$\pi$ level lengthens the NO bond and decreases the NO stretch frequency compared to gas phase NO. We calculate the normal mode NO stretch frequency in CuNO to be 1648 cm$^{-1}$, which is in reasonable agreement with the experimental Ar matrix isolation result (1611 cm$^{-1}$).[67] In [CuNO]$^+$, formally no charge transfer occurs and the N−O bond length and stretch frequency (Table 2) are very close to their gas phase values of 1.15 Å and 1876 cm$^{-1}$, respectively. The NO 2$\pi$ orbital is populated in both CuNO and [CuNO]$^+$; as with CuCO, rehybridization of the 2$\pi$ orbital with the Cu 4s orbital provides the driving force for the bending of NO in these two cases. In [CuNO]$^{2+}$, a partial charge transfer from the NO 2$\pi$ level to the incompletely filled Cu d level results in a shorter NO bond[27] and higher NO stretch frequency than those of gas phase NO. [CuNO]$^{2+}$ is isoelectronic with [CuCO]$^+$, and, like the latter, is linear.

In water ligand models, the nominal Cu oxidation state is again the most important influence on the calculated NO stretch frequency, with a higher oxidation state resulting in a higher frequency. Additional coordination has a secondary, but significant, effect comparable to that found for the carbonyl complexes. Regardless of the oxidation state, as coordination increases and the Cu center becomes more electron rich, the NO bond lengthens and the NO stretch frequency decreases. Bending also affects the NO bond length and frequency. We expect and find NO to bend in all the nominal Cu(0) and Cu(I) complexes, but surprisingly, as the Cu coordination increases, bending becomes favorable for the Cu(II) complexes as well. While dismissed in our earlier studies,[27,28] this bending is likely a real effect arising from second-order Jahn−Teller interactions between occupied Cu d and vacant NO 2$\pi$ orbitals that become increasingly important as the coordination increases and the energy separation between the two orbital sets decreases. Bent and linear results for NO on Cu(II) are listed in Table 2. NO bending results in an increased occupation of the antibonding NO 2$\pi$ level and thus an increase in NO bond length and decrease in NO stretch frequency (by up to 70 cm$^{-1}$).

The nominal Cu(I) water ligand models and comparable purely siliceous models yield similar geometries and vibrational frequencies (Tables 2 and 4). As with the carbonyl systems, reducing the overall cluster charge and increasing the electron donation to Cu by introducing either Al or hybrid J atoms into the larger models results in a systematic decrease in calculated frequencies. The coordination and cluster charge effects are comparable in magnitude and difficult to separate in the Cu(I) models. In fact, for the larger ring models of Cu(I), the symmetry reduction accompanying bending allows the Cu center to move closer to two oxygen atoms, so that the framework coordination is ill-defined but certainly less than four. This effect is particularly pronounced in the nominally 4-coordinated [Cu($Si_5AlO_6H_{12}$)NO] complex, in which the Cu ion clearly moves to a 2-coordinate location over the Al T-site and illustrates the influence of the Al location on Cu coordination.

The coordination number and the *nature* of the model coordination environment have distinctive influences on the NO stretch frequencies in Cu(II) systems. The NO frequencies for linear and bent [Cu($Si_6O_6H_{12}$)NO]$^{2+}$ (nominally Cu(II)) are more than 90 cm$^{-1}$ less than those of [Cu($H_2O$)$_4$NO]$^{2+}$. Introducing two Al atoms in the larger Cu(II) model reduces the NO vibrational frequency even further, so that the 1- to 4-coordinated Cu(II)−NO water ligand models and the larger charged and neutral Cu(II)−NO models span separate regions of the vibrational spectrum.

Figure 6 shows a plot of the EFFF NO stretch frequency vs the N−O bond length for both water ligand and larger model complexes. Unlike the monocarbonyl complexes, three distinct frequency regimes are observed corresponding to nominal Cu(0), Cu(I), or Cu(II) (*i.e.*, effectively [Cu(I)−NO$^-$], [Cu(I)−NO], or [Cu(I)−NO$^+$], respectively). An almost linear correlation, independent of the cluster charge, binding mode of NO (linear or bent), and details of the local coordination environment of Cu, is observed with an overall fit quality of 0.9910. Here again the data point corresponding to gas phase NO, which was not used in the fitting procedure, lies close to the best fit line. Comments that were made earlier about the predictive nature of a similar plot for carbonyl complexes apply here as well. The N−O bond lengths and frequencies span a much greater range and are thus much more sensitive to model choice than was the case with carbonyl complexes. This greater sensitivity is consistent with the increased charge transfer and greater covalency in the Cu−NO bond than in the Cu−CO bond.

In Figure 6, we also show frequency ranges corresponding to absorptions that have been assigned to NO adsorbed on Cu(I) and Cu(II) sites in zeolites.[4−11] The two ranges are separated by 100 cm$^{-1}$, with the higher one assigned to NO on Cu(II) and the lower one to NO on Cu(I). These assignments are consistent with our model results. For Cu(I), both water ligand

and larger models produce frequencies in the range of the experimental results; both are reasonable models of Cu(I) sites in Cu-exchanged zeolites. Again, given the uncertainties associated with the overall computational method and models, we cannot unequivocally associate the experimental frequencies with any one coordination model considered here. For Cu(II), the larger models clearly produce frequencies that are most consistent with the experimental results, while the water ligand models produce frequencies that are consistently too large. As noted in the Introduction, bands at 1895 and 1912 $cm^{-1}$ have been assigned to the stretching modes of NO bound to $Cu^{2+}$ near one and two framework Al, respectively.[7,8] The trends we observe in frequency vs local coordination environment suggest the opposite assignment. However, an additional factor that may be important in these and all Cu(II) vibrational frequency assignments is the presence of extralattice $O^-$ and/or $OH^-$. Extralattice oxygen is thought to be important in charge compensating Cu(II), particularly in overexchanged zeolites.[2,16] While we have not explored the effects of extralattice oxygen in detail, we have found that inclusion of an $OH^-$ ligand in the Cu coordination sphere can shift CO and NO stretch frequencies downward in the same way that Al or hybrid J atoms do. For this and the reasons listed above, we hesitate to associate one particular Cu(II) coordination model with Cu(II) in ZSM-5.

**D. $Cu^{n+}$-Bound Dinitrosyl $[Cu(H_2O)_x(NO)_2]^{n+}$ Complexes.** On a variety of transition metal oxide surfaces and transition metal ion-exchanged zeolites, NO has a strong tendency to adsorb in pairs.[68,69] This tendency has been ascribed to enhanced stability gained by the interaction of the unpaired electron on each of the NO ligands.[70] Dinitrosyl species have been observed experimentally when the reduced forms of Cu−ZSM-5 or Cu−Y (containing predominantly Cu(I)) are exposed to NO.[4−11] Also, dinitrosyl species have been suggested to play a role in the mechanism of NO decomposition.[2,9,10,11] We describe here the results that we obtained from vibrational frequency calculations on dinitrosyl complexes within the framework of our water ligand model. The calculated symmetric and antisymmetric dinitrosyl stretch frequencies for these complexes, along with experimentally observed frequencies in Cu-exchanged zeolites,[4−11] are collected in Table 6. For Cu(I) complexes, frequency calculations were performed only for singlet ($^1A_1$) states, which were the ground states. Preliminary Hartree−Fock calculations[31] for nominal Cu(I)-bound dinitrosyl species yield symmetric and antisymmetric NO stretch frequencies of 1646 and 1578 $cm^{-1}$, respectively. These values significantly underestimate the observed dinitrosyl frequencies in Cu-exchanged zeolites (by over 150 $cm^{-1}$), even without allowing for a further reduction by a typical Hartree−Fock scaling factor (≈0.89[50]).

Cu in the dinitrosyl complexes, as in mononitrosyl complexes, has a strong propensity to remain in an effective Cu(I) oxidation state, irrespective of the overall charge and degree of coordination.[44] Dinitrosyl binding to $Cu^0$, $Cu^+$, and $Cu^{2+}$ can be approximately represented as $[Cu(I)-(NO)_2^-]$, $[Cu(I)-(NO)_2]$, and $[Cu(I)-(NO)_2^+]$, respectively, so that across the series electrons are removed from orbitals of NO $2\pi$ origin. The N−O bond lengths and vibrational frequencies of the dinitrosyl species are consonant with this view of charge transfer. In the case of $[Cu(NO)_2]^+$, with effectively neutral $(NO)_2$, the calculated scaled symmetric and antisymmetric normal mode NO stretch frequencies (1869 and 1798 $cm^{-1}$, respectively) and bond length (1.14 Å) are even in surprisingly good agreement with the observed gas phase bare NO dimer frequencies of 1860−1870 and 1760−1788 $cm^{-1}$ [54,71] and bond length of 1.16 Å. In the more reduced

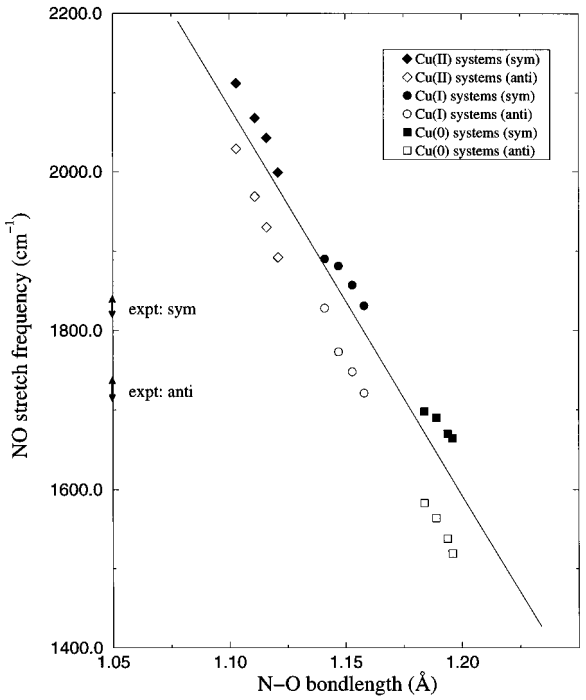


**Figure 7.** Calculated symmetric and antisymmetric NO frequencies (from EFFF method, scaled by 0.97) vs N−O bond lengths for dinitrosyl $[Cu(H_2O)_x(NO)_2]^{n+}$ complexes. Linear fit to mononitrosyl results (from Figure 6) and ranges of experimental values (Table 6) are also shown.

$Cu(NO)_2$ systems, the N−O bond lengths are increased and vibrational frequencies decreased, while for the more oxidized $[Cu(NO)_2]^{2+}$ systems, the opposite trend is observed. As before, higher Cu coordination has the effect of decreasing frequencies and increasing bond lengths. Regular correlations are again observed (Figure 7) between the N−O bond lengths and EFFF NO frequencies for Cu-bound dinitrosyl complexes. As in dicarbonyl systems, the averages of the symmetric and antisymmetric NO stretch frequencies lie reasonably close to the straight line taken from the fit to the corresponding mononitrosyl results in Figure 6. The splitting between the two stretch modes again decreases with increasing Cu oxidation state, but by a much smaller amount than in dicarbonyl complexes, presumably because the bonding combination of $2\pi$ orbitals is always at least singly occupied in dinitrosyl complexes.

Experimentally observed frequencies[4−11] that have been previously assigned to symmetric and antisymmetric modes of dinitrosyl species adsorbed at Cu(I) sites in Cu−ZSM-5 and Cu−Y zeolites are also indicated in Figure 7. The present calculations reinforce this interpretation, as only the calculated frequencies for Cu(I) complexes are in reasonable agreement with the experimentally observed frequencies. The above experience with monocarbonyl and mononitrosyl species suggests that this assessment would persist even if the simple water ligand models considered in this section were supplemented with results for larger clusters. The present Cu(I) results are also consistent with the frequency ranges of 1810−1940 and 1685−1815 $cm^{-1}$, which have been assigned to symmetric and antisymmetric NO stretch frequencies, respectively, for dinitrosyl species adsorbed on other transition metal ion exchanged zeolites and on supported and unsupported transition metal oxides.[68] This indicates that the mode of dinitrosyl binding found here for $Cu^+$ complexes, *viz.*, $[Cu(I)-(NO)_2]$ (with the dinitrosyl remaining more or less neutral), is probably the preferred mode in most other systems as well.

## IV. Summary and Conclusions

The lack of definitive experimental information on the location and oxidation state of exchanged Cu ions in zeolites has led us to develop cluster models of Cu(0), Cu(I), and Cu(II) sites with varying degrees of local coordination at various levels of sophistication.[27,28] In the present study, we have presented a set of CO and NO vibrational frequency calculations for Cu-bound mono- and dicarbonyl and mono- and dinitrosyl complexes. We have shown that the results of these calculations can be combined with available IR experimental measurements both to assess the reliability of our models and to help interpret experimental observations. In general, our models yield CO and NO stretch frequencies in ranges that are quite consistent with IR measurements. In all cases, our calculations reinforce previous assignment of the observed frequencies.

We have identified several factors that affect the CO and NO stretch frequencies:

1. In general, a lower nominal Cu oxidation state results in lower CO and NO frequencies. Because mono- and dinitrosyl species interacting with Cu(0), Cu(I), and Cu(II) can be approximately described as $[Cu(I)-(NO)_x^-]$, $[Cu(I)-(NO)_x]$, and $[Cu(I)-(NO)_x^+]$, $x = 1, 2$, respectively, three distinct frequency regimes are observed for nitrosyl complexes, one for each charged state of the adsorbed $(NO)_x$ species. The dependence on oxidation state is less dramatic in the case of carbonyl complexes; Cu(I) and Cu(II) complexes display CO stretch frequencies in overlapping ranges (due to similar extent of charge transfer between CO and Cu in these two cases).

2. A higher degree of Cu coordination has the secondary, but significant, effect of lowering the CO and NO frequencies. The Cu center becomes a better electron donor and poorer electron acceptor as its coordination number increases, resulting in a greater charge transfer to CO and NO, an increase in the C−O and N−O bond lengths, and a decrease in stretch frequencies.

3. More sophisticated zeolite models generally result in lower CO and NO stretch frequencies. The frequency trends can be summarized by:

$$\nu_{CO,NO}^{waterligand} \geq \nu_{CO,NO}^{larger(siliceous)} > \nu_{CO,NO}^{larger(withAlorJ)}$$

where the equal sign is for Cu(I) systems. The overall frequency range is much broader for Cu(II) than for Cu(I) systems, with a much greater disparity between water ligand and larger models in the former case. The water ligand models may provide a reasonable description of Cu(I) sites in zeolites, but more sophisticated models may be required to study the Cu(II) sites.

4. In the mononitrosyl complexes, NO bending lowers the NO stretch frequency.

Despite the large variations in NO and CO stretch frequencies that occur in our models, we find very strong linear correlations between calculated frequencies and bond lengths for each class of adsorbates considered. These correlations and the above trends should prove useful in future studies of Cu-exchanged zeolites.

**Acknowledgment.** The authors thank M. Shelef (Ford Motor Co.) for useful discussions, T. A. Barckholtz (Ohio State University) for assistance with the EFFF method, and the authors of refs 31 and 32 for sending preprints prior to publication. R.R. and J.B.A. would like to acknowledge support by NSF under Grant NSF-1-5-30897 (8), the National Center for Supercomputing Applications (NCSA), the Cornell Theory Center (CTC), and two summer appointments for R.R. at the Ford Research Laboratory.

## References and Notes

(1) (a) Iwamoto, M.; Mizuno, N. *J. Automot. Eng. (Part D Proc. Inst. Mech. Eng.)* **1993**, *207*, 23. (b) Iwamoto, M.; Hamada, H. *Catal. Today* **1991**, *10*, 57. (c) Iwamoto, M.; Mizuno, N. *Proc.—Inst. Mech. Eng.* **1993**, *207*, 23.

(2) Shelef, M. *Chem. Rev.* **1995**, *95*, 209.

(3) Centi, G.; Perathoner, S. *Appl. Catal. A* **1995**, *132*, 179.

(4) Hoost, T. E.; Lafromboise, K. A.; Otto, K. *Catal. Lett.* **1996**, *37*, 153.

(5) Cheung, T.; Bhargava, S. K.; Hobday, M.; Foger, K. *J. Catal.* **1996**, *158*, 301.

(6) Beutel, T.; Sárkány, J.; Lei, G.-D.; Yan, J. Y.; Sachtler, W. M. H. *J. Phys. Chem.* **1996**, *100*, 845.

(7) Aylor, A. W.; Larsen, S. C.; Reimer, J. A.; Bell, A. T. *J. Catal.* **1995**, *157*, 592.

(8) Dědeček, J.; Sobal'ik, Z.;Tvaružková, Z.; Kaucký, D.; Wichterlová, B. *J. Phys. Chem.* **1995**, *99*, 16327.

(9) Spoto, G.; Zecchina, A.; Bordiga, S.; Ricchiardi, G.; Martra, G. *Appl. Catal. B: Environ.* **1994**, *3*, 151.

(10) Valyon, J.; Hall, W. K. *J. Phys. Chem.* **1993**, *97*, 1204.

(11) Giamello, E.; Murphy, D.; Magnacca, G.; Morterra, C.; Shioya, Y.; Nomura, T.; Anpo, M. *J. Catal.* **1992**, *136*, 510.

(12) Hoost, T. E.; Lafromboise, K. A.; Otto, K. *Catal. Lett.* **1995**, *33*, 105.

(13) Komatsu, T.; Ogawa, T.; Yashima, T. *J. Phys. Chem.* **1995**, *99*, 13053.

(14) Iwamoto, M.; Yahiro, H.; Mizuno, N.; Zhang, W. X.; Mine, Y.; Furukawa, H.; Kagawa, S. *J. Phys. Chem.* **1992**, *96*, 9360.

(15) Yamashita, H.; Matsuoka, M.; Tsuji, K.; Shioya, Y.; Anpo, M. *J. Phys. Chem.* **1996**, *100*, 397.

(16) Petunchi, J. O.; Marcelin, G.; Hall, W. K. *J. Phys. Chem.* **1992**, *96*, 9967.

(17) Anderson, M. W.; Kevan, L. *J. Phys. Chem.* **1987**, *91*, 4174.

(18) Kucherov, A. V.; Hubbard, C. P.; Shelef, M. *J. Catal* **1995**, *157*, 603.

(19) Slinkin, A. A.; Kucherov, A. V.; Chuylkin, N. D.; Korsunov, V. A.; Klyachko, A. L.; Nikishenko, S. B. *Kinet. Katal.* **1990**, *31*, 698.

(20) Kucherov, A. V.; Slinkin, A. A. *J. Phys. Chem.* **1989**, *93*, 864.

(21) Kucherov, A. V.; Slinkin, A. A.; Kondrat'ev, D. A.; Bondarenko, T. N.; Rubinstein, A. M.; Minachev, Kh. M. *Zeolites* **1985**, *5*, 320.

(22) Larsen, S. C.; Aylor, A.; Bell, A. T.; Reimer, J. A. *J. Phys. Chem.* **1994**, *98*, 11533.

(23) Hamada, H.; Matsubayashi, N.; Shimada, H.; Kintaichi, Y.; Ito, T.; Nishijima, A. *Catal. Lett.* **1990**, *5*, 189.

(24) Liu, D.-J.; Robota, H. J. *Catal. Lett.* **1993**, *21*, 291.

(25) Liu, D.-J.; Robota, H. J. *Appl. Catal.* **1994**, *4*, 155.

(26) Grünert, W.; Hayes, N. W.; Joyner, R. W.; Shpiro, E. S.; Siddiqui, M. R.; Baeva, G. N. *J. Phys. Chem.* **1994**, *98*, 10832.

(27) Schneider, W. F.; Hass, K. C.; Ramprasad, R.; Adams, J. B. *J. Phys. Chem.* **1996**, *100*, 6032.

(28) Hass, K. C.; Schneider, W. F. *J. Phys. Chem.*, **1996**, *100*, 92992.

(29) Trout, B. L.; Chakraborty, A. K.; Bell, A. T. *J. Phys. Chem.* **1996**, *100*, 4173.

(30) Yokomichi, Y.; Ohtsuka, H.; Tabata, T.; Okada, O.; Yokoi, Y.; Ishikawa, H.; Yamaguchi, R.; Matsui, H.; Tachibana, A.; Yamabe, T. *Catal. Today* **1995**, *23*, 431.

(31) Trout, B. L.; Chakraborty, A. K.; Bell, A. T. *J. Phys. Chem.* **1996**, *100*, 17582.

(32) Brand, H. V.; Redondo, A.; Hay, P. J. Unpublished results.

(33) Zygmunt, S. A.; Curtiss, L. A.; Iton, L. E.; Erhardt, M. K. *J. Phys. Chem.* **1996**, *100*, 6663.

(34) Bishop, D. M.; Cybulski, S. M. *Chem. Phys. Lett.* **1994**, *230*, 177.

(35) Koubi, L.; Blain, M.; de Lara, E. C. *Chem. Phys. Lett.* **1994**, *217*, 544.

(36) Pelmenschikov, A. G.; van Santen, R. A. *J. Phys. Chem.* **1993**, *97*, 10678.

(37) Gale, J. D.; Catlow, C. R. A.; Carruthers, J. R. *Chem. Phys. Lett.* **1993**, *216*, 155.

(38) Brand, H. V.; Curtiss, L. A.; Iton, L. E. *J. Phys. Chem.* **1992**, *96*, 7725.

(39) Sárkány, J.; d'Itri, J.; Sachtler, W. M. H. *Catal. Lett.* **1992**, *16*, 241.

(40) Chajar, Z.; Primet, M.; Praliaud, H.; Chevrier, M.; Gauthier, C.; Mathis, F. *Appl. Catal. B: Environ.* **1994**, *4*, 199.

(41) Baerends, E. J.; Ellis, D. E.; Ros, P. *Chem. Phys.* **1973**, *2*, 41.

(42) Bérces, A.; Ziegler, T. *J. Phys. Chem.* **1993**, *98*, 4793.

(43) Vosko, S. H.; Wilk, L.; Nusair, M. *Can. J. Phys.* **1980**, *58*, 1200.

(44) Ramprasad, R.; Hass, K. C.; Schneider, W. F.; Adams, J. B. Unpublished results.

(45) Braterman, P. S. *Metal Carbonyl Spectra*; Academic Press: New York, 1975.

(46) Cotton, F. A.; Kraihanzel, C. S. *J. Am. Chem. Soc.* **1962**, *84*, 4432.

(47) Wilson, E. B, Jr.; Decius, J. C.; Cross, P. C. *Molecular Vibrations: The Theory of Infrared and Raman Vibrational Spectra*; McGraw-Hill Book Company: New York, 1955; Chapter 4.
(48) Post, D.; Baerends, E. J. *Chem. Phys.* **1983**, *78*, 5663.
(49) Rauhut, G.; Pulay, P. *J. Phys. Chem.* **1995**, *99*, 3093.
(50) Pople, J. A.; Scott, A. P.; Wong, M. W.; Radom, L. *Isr. J. Chem.* **1993**, *33*, 345.
(51) Bauschlicher, C. W. *Chem. Phys. Lett.* **1995**, *246*, 40.
(52) *CRC Handbook of Chemistry and Physics*; 63rd ed., Weast, R. C, ed., CRC Press: Boca Raton, FL, 1982.
(53) Huber, K. P.; Herzberg, G. *Molecular Spectra and Molecular Structure. IV. Constants of Diatomic Molecules*; Van Nostrand Reinhold: Toronto, 1979.
(54) Laane, J.; Ohlsen, J. R. *Prog. Inorg. Chem.* **1980**, *27*, 465.
(55) Chenier, J. H. B.; Hampson, C. A.; Howard, J. A.; Mile, B. *J. Phys. Chem.* **1989**, *93*, 114.
(56) Huber, H.; Kündig, E. P.; Muskovits, M.; Ozin, G. A. *J. Am. Chem. Soc.* **1975**, *97*, 2097.
(57) Fournier, R. *J. Chem. Phys.* **1995**, *102*, 5396.
(58) Fournier, R. *J. Chem. Phys.* **1993**, *98*, 8041.
(59) Schwerdtfeger, P.; Bowmaker, G. A. *J. Chem. Phys.* **1994**, *100*, 4487.
(60) Bauschlicher, C. W. *J. Chem. Phys.* **1994**, *100*, 1215.
(61) Barone, V. *Chem. Phys. Lett.* **1995**, *233*, 129.
(62) Sodupe, M.; Bauschlicher Jr., C. W.; Lee, T. J. *Chem. Phys. Lett.* **1992**, *189*, 266.
(63) Barnes, L. A.; Rosi, M.; Bauschlicher Jr., C. W. *J. Chem. Phys.* **1990**, *93*, 609.
(64) Ogletree, D. F.; Van Hove, M. A.; Somorjai, G. A. *Surf. Sci.* **1986**, *173*, 351.
(65) Kampshoff, E.; Hahn, E.; Kern, K. *Phys. Rev. Lett.* **1994**, *73*, 704.
(66) Barone, V. *J. Phys. Chem.* **1995**, *99*, 11659.
(67) Chiarelli, J. A.; Ball, D. A. *J. Phys. Chem.* **1994**, *98*, 12828.
(68) Kung, M. C.; Kung, H. H. *Catal. Rev.* **1985**, *27* (3), 425.
(69) Portella, L.; Grange, P.; Delmon, B. *Catal. Rev.—Sci. Eng.* **1995**, *37* (4), 699 and references therein.
(70) Zecchina, A.; Garrone, E.; Morterra, C.; Coluccia, S. *J. Phys. Chem.* **1975**, *79*, 978.
(71) Dinerman, C. E.; Ewing, G. E. *J. Chem. Phys* **1970**, *53*, 626.